The effect of crystallization level of silica nanoparticles on cell proliferation of MRC-5 cell line and its prediction using artificial neural network

Fariba Abbasi
Shiraz University of Medical Sciences
Mohammad Reza Samaei (mrsamaei@gmail.com)
Department of Environmental Health Engineering, Shiraz University of medical science, Shiraz, Iran
Hassan Hashemi
Shiraz University of Medical Sciences
Amir Savardashtaki
Shiraz University of Medical Sciences
Abolfazl Azhdarpoor
Shiraz University of Medical Sciences
Mohammad Javad Fallahi
Shiraz University of Medical Sciences
mahrokh jalili
Shahid Sadoughi University of Medical Sciences and Health Services Yazd Research and Clinical Centre for Infertility
Sylvain Billet
Universite du Littoral Cote D'Opale

Research

Keywords: SiO2 NPs, temperature calcination, cell proliferation, artificial neural network

Posted Date: March 24th, 2020

DOI: https://doi.org/10.21203/rs.3.rs-18704/v1

Abstract

Background: This study investigated the effect of the level of silica nanoparticles (SiO_2NPs) crystallization on the cell proliferation of MRC-5 cells and its prediction using an artificial neural network (ANN).

Methods: Variables studied included temperature (70-1000°C), calcination time (2, 12 and 24 hours), and catalyst feed rate (0.01, 0.05 and 0.1mL/min). Cell proliferation was determined by the MTT test after 24 hours of exposure, and results were analyzed using the t-test in MATLAB.

Results: the synthesized particles size was less than 50nm, and the XRD peak varied from 30 to 21° during the increase in calcination temperature. The maximum level of crystallization was at 800°C (58% relative to amorphous) with the lowest cell viability. Cell proliferation decreased with increasing concentration of nanoparticles ($p<0.05$) and increasing feed rate. There was also a positive relationship between increased crystallization and decreased cell proliferation (R^2=0.78), but no such association was observed for calcination time. Cell proliferation of MRC-5 was slightly correlated with the linear regression model (MSE>0.12), while ANN was well predicted by the Levenberg–Marquardt algorithm. The suggested structure in this study was 4:10:1 with R^2_{all}=0.97, R^2test=0.97, RMSE=0.25 and MSE=0.003. The correlation between laboratory results and ANN prediction was 0.94, and the minimum and maximum OD level in the laboratory data and predicted ANN were attributed to 20 and 13 runs.

Conclusion: changes in the degree of crystallization of SiO_2NPs, an increase in concentration, and the rate of catalyst feed during crystallization of SiO_2NPs were practical factors in increasing cytotoxicity.

1. Introduction

SiO_2 nanoparticles (NPs) are one of the most common and widely used nanomaterials in industrial and medical fields such as drug delivery, biosensors, cancer treatment, environmental sensors and dispersion of solvent including toluene in industries resulting in increased environmental and occupational exposure (1). SiO_2 NPs are usually available in either amorphous or crystalline forms, the former being classified as industrial environmental products and the latter as natural environmental pollutants. The SiO_2 NPs are initially colloidal, which become amorphous during synthesis and then crystallized by calcination (2). During this process, the amorphous SiO_2 NPs have a long-range order in their crystalline structure and form tetra and hexagonal crystals. Although during the silica crystallization process due to the increase in effective nucleation function of silica, the crystallization of SiO_2 NPs increases (3), but several factors are involved in the SiO_2 NPs crystallization, such as temperature, time, pressure, size of nanoparticles, water content, percentage of elements such as NaCl, addition of calcifying agents, silicatein filaments (4-7). But it can be said that temperature is one of the most effective and practical factors in the crystallization of many nanoparticles, including silica, whose role in hydrothermal synthesis has been shown to increase their crystallization (8). In many glass and ceramic industries, the crystallization of silica compounds is

also carried out by temperature (9). Because of its nature, silica is toxic to human cells, but if it is nano-sized, its toxicity is exacerbated. Previous studies have shown the toxicity of deposited, colloidal, pyrogenic, and crystalline silica on human and mouse cells (10-13). Although the mechanisms of toxicity of amorphous and crystalline nanoparticles are similar (14), changes in the structure of the material occur during the crystallization process of silica. This could affects many of its properties such as physicochemical ones, biological behavior, and cytotoxicity. SiO_2 NPs penetrate in the plasma membrane at a very tiny size (less than 10 nm) because of their smaller size than the cellular organs, and deposits in the mitochondria or even on the nucleus, and induce the cell death (1). A 24-hr exposure of lung fibroblast cells to SiO_2 NPs is able to induce genotoxicity and cell death (10, 12, 15, 16). The cytotoxicity of SiO_2 NPs depends on their crystallinity. Thus, in occupational studies, exposure to crystalline silica has been shown to cause silicosis and lung disease (17). However, insufficient attention has been paid to the degree of crystallization and the effect of the crystallization process on the cytotoxicity of SiO_2 NPs. In addition, prediction of these effects on lung cells is another aspect of the studies that can be investigated by non-linear, and in some cases, linear modelling. Among the models, in the case of a multi-agent intervention, the artificial neural network has great power in predicting effects. The objectives of this study was to investigate the effect of SiO_2 NP crystallization rate on cell proliferation in human pulmonary fibroblast (MRC-5) and its prediction using artificial neural networks.

2. Material And Methods

2.1. Materials

Materials used include tetraethoxysilane (TEOS 98%, Merck Germany), pure ethyl alcohol (ethanol, Merck Germany), ammonia 25% (Merck Germany), 3-(4,5-dimethylthiazol-2-yl)-2,5-diphenyltetrazolium bromide (MTT, Sigma USA), Dimethyl sulfoxide (DMSO, Merck Germany), Dulbecco modified Eagle's minimal essential medium (DMEM, Gibco England) + Glutamax (high glucose), Fetal Bovine Serum (FBS, Merck Germany), Penicillin Streptomycin Solution (pen-strep, Merck Germany) trypsin 0.025% - EDTA (1x, Merck Germany) and deionized water (Merck Germany) were used.

2.2. Synthesis of SiO_2 Nanoparticles

Due to the high homogeneity and purity of the sol-gel method, this method has been used for the synthesis of nanoparticles (18) based on the Stober method. According to this method, under ultrasonic conditions, (40 kHz) 5 ml of TEOS was dissolved in 30 ml of ethanol for 10 min. Then, to facilitate ionization, 2 ml of distilled water was added to the solution at a feed rate = 0.2 ml/min under ultrasonic conditions. After 1.5 h, ammonia was added as a catalyst at feed rate = 0.01 ml/min and sonicated for 3 h to obtain a gelatin solution.

Subsequently, for aging, the sample was kept under ambient conditions (1h) and finally washed with ethanol and distilled water, 3 × 7000 rpm (g-force = 5478.2). The product was dried for 24 h at 70 °C and then crystallized at different temperatures (350, 600, 800, and 1000 °C). The degree of crystallization of

the nanoparticles was evaluated by X-ray dispersion (XRD). Then, Field emission scanning electron microscopy (FESEM) coupled to energy dispersive spectroscopy (EDS) was used to determine the size and purity of NPs. Finally, the distribution of nanoparticles in solution was determined by Dynamic light scattering (DLS).

2.3. Cell culture

Human fibroblastic lung cells (MRC-5) were purchased from Iran Genetics Resource Center. The cell line was cultured under standard conditions (37 °C, 5% of CO_2, and 90% of humidity). The used medium culture was DMEM enriched with 15% of FBS and 1% pen-strep. Experiments were performed at the passage of 3 after opening from the nitrogen tank.

2.4. MTT assay

Cell proliferation was evaluated by studying the mitochondrial dehydrogenase activity in MRC-5 cells. A number of 15,000 cells/well were cultured in a 96-well plate that cultured for 48 h before exposure. The cells were exposed to 0.06, 0.1, 0.6, 6 or 60 mg of SiO2 NPs/ml during 24h. Unexposed cells were used as negative controls (100% viability). The MTT assay was performed according to the manufacturer's instructions. Briefly, 10µl of MTT was added to each well. After 4 h, the light absorption was measured at 570 nm wavelengths.

2.5. Statistical analysis

Descriptive statistics were used to determine cellular viability. The cellular viability at each exposure concentration and each nanoparticles were calculated using the one-way ANOVA test. Correlation between cellular viability and variables was analyzed by Spearman, and the significance level was set at 0.05. Then linear and nonlinear regression tests were applied to improve its mathematical model to determine the effect of calcination temperature on the nanoparticles. Statistical analyses were performed using Matlab 2018.

2.6. ANN modelling

ANN is one of the modeling methods for determining the non-linear relationship between the variables, which was carried out in this study by feed-forward backpropagation and Matlab 2018 (19). In the neural network, there are several inputs, the hidden layer, and the output, in which the number of neurons in each hidden layer has a very important response. In addition, the relationship between the layers is determined by the assigned weight. Initially, the network is trained with derived laboratory data from cell viability, of which 70, 15, and 15% of the data are used for training, validation, and testing, respectively. Subsequently, the training was used to determine the weight and bias, thus controlling the validation error rate. Then, the training was stopped to avoid an over-fitting increase when the validation error was increased by special iterations (20). Given the significance and accuracy of the mean square error (MSE) and correlation coefficient (R), the best ANN structure for predicting cell proliferation in MRC-5 exposed to SiO_2 NPs,

based on MSE and R from the number of neurons, in the hidden layer recommended. The number of neurons in the hidden layer is determined by two equations 1 and 2:

$$\frac{2(i+o)}{3} < n < i(i+o) - 1 \quad (1)$$

$$0.5i-2<n<2i+2 \quad (2)$$

i=number of inputs, o= the number of outputs and n=number of hidden layer neuron.

3. Result And Discussion

3.1. Characterization of SiO_2 NPs

In this study, due to the effect of calcination temperature on the crystallization of nanoparticles (21), the crystallization process of SiO_2 NPs during calcination temperature increase from 70-1000 °C was investigated. As the calcination temperature increased, the maximum angle in the XRD diagram varied from 23° in sample A (dried at 70 °C) to nearly 30° at 800 °C (Fig. S1). Because drying occurred at low temperature (70-150 °C), at which temperature the silica was amorphous (22). In previous studies, the XRD peak for amorphous and crystalline SiO_2 NPs was also 14-21 and 26-27°, respectively (7, 23, 24). Also, the degree of crystallization, XRD peak and mean diameter of nanoparticles in aqueous media by DLS, and weight percent of elements in SiO_2 NPs by EDS during calcination temperature increase is shown in Table 1.

Table 1. Crystalline degree based on calcination temperature. A: 70 °C; B: 350 °C; C: 600 °C; D: 800 °C and E: 1000 °C

		A	B	C	D	E
The ratio of crystallization to amorphous		1	1.07	1.17	1.22	1.38
Diameter in DLS		>1000 nm	47.4 nm	40.2 nm	35.3 nm	32 nm
A percent of Si, O and C from EDS	Si	22.72	24.35	25.57	29.12	35.55
	O	76.2	75.65	74.43	70.88	64.45
	C	1.8	-	-	-	-

According to Table 1, the highest crystallization rate was in E nanoparticles (calcinated at 1000 °C). The crystallization rate was 38% compared to the amorphous sample. In other studies, crystallization has been observed at different temperatures according to the synthesis conditions. In the study of Fuchs et al., 2014, in the presence of calcinats, the temperature required for the conversion of silica to cristobalite was at 850 °C (7). However, under the continuous addition of these agents, the synthesis temperature of quartz was reduced to 200 °C. The EDS results also show that only the amorphous silica nanoparticles have a carbon peak (table 1). Because within 24 h at 70 ° C, many mineral carbon compounds are not volatile (25) However, because the crystallization of silica is well performed, the crystals contain only

silica and oxygen (26). Thus, the presence of only Si and O peaks at temperatures of 350, 600, 800, and 1000 °C indicates the appropriate crystallization of the nanoparticles. On the other hand, the FESEM images of all the nanoparticles have shown the size <50nm of all the nanoparticles. Whereas DLS has shown that most amorphous nanoparticles because of rapidly agglomeration due to their high surface area and reactivity, resulting in differences in primary and secondary size (27, 28). So that particle size reached above 1000 nm, whereas for B-E samples, the mean particle size was <50 nm. Although the results of Table 1 show the process of crystallization of nanoparticles, the increase in temperature did not have a significant effect on the crystallization of silica. Thus, the increase in calcination time was used as a variable to increase the crystallization of the silica, the results of showed increasing of degree for the XRD peak from 2 h to 24 h of calcination time. Thus, the crystallization of nanoparticles increased as calcination time increased. That, the crystallization of SiO_2 NPs at 1000 °C during 24 h was longer because there is sufficient opportunity for the development of regular SiO_2 crystals with increasing time.

3.2. The effect of the feed rate of catalyst on the crystallinity of SiO_2 NPs

In this study, used silica nanoparticles were smaller than 50 nm. Because smaller sizes of nanoparticles are more likely to penetrate the cell. Due to the effect of the feed rate of catalyst on nanoparticle size (29), crystallization level, purity percentage, size in aqueous media, and XRD peak degree at feed rates of 0.01, 0.05 and 0.1 ml/min are shown in Table 2, respectively.

Table 2. The level of Crystallization SiO_2 NPs based on the feed rate of catalyst

Nanoparticles	F (0.01 ml/min)	G (0.05 ml/min)	H (0.1 ml/min)
The ratio of crystallization to amorphous	1.55	1.115	1.0127
Diameter in DLS	<50 nm	<50 nm	<50 nm

According to Table 2, the rate of crystallization of nanoparticles decreased with increasing feed rate. So that the maximum crystallization was at feed rate = 0.01 ml/min. Because higher feed rates do not provide sufficient time for the catalytic reaction, and because of the lower surface-area-to-volume ratio of catalyst droplets, many TEOS molecules may remain unchanged. FESEM and DLS also showed particle size <50nm under these conditions. Because these nanoparticles are calcinated at high temperatures, which made them crystallize, and as a result, their agglomeration has decreased.

3.3. Toxicity of SiO_2 NPs on MRC-5

3.3.1. Toxicity of SiO_2 NPs based on calcination temperature

In this study, cellular viability due to exposure of MRC-5 to synthesized SiO_2 NPs at various temperatures, times of calcination, and different feed rates, were determined by the MTT test, as shown in Fig. 1, 2 and 3, respectively.

As shown in Fig. 1, the MRC-5 cell proliferation rate decreased with increasing concentration of nanoparticles. The minimum cell proliferation rate was observed in all nanoparticles at a concentration of 60 mg/ml ($p < 0.05$). Because the toxicity of in vitro nanoparticles depends on the concentration dose, size of nanoparticles, and cell type (14, 30, 31). In general, at concentrations above 100 µg/ml, it had toxic effects on MRC-5. In a study of Yang et al., 2019, cytotoxicity at concentrations above 25 µg/ml of silica nanoparticles also had toxic effects on HL-7702. HFL-1 cell viability also decreased with an increasing concentration of 250–1500 µg/ml (32). Also, the lethality at 600 µg/ml concentration was higher than 60µg/ml ($p = 0.01$). In a study by Petrache Voicu et al., 2015, cell viability also decreased dramatically with increasing nanoparticle concentrations, from 12 to 62 µg/ml. Cytoplasmic vacuolization was also observed at concentrations above 60 µg/ml. Because at higher concentrations, the cell is more likely to be exposed to nanoparticles (16). According to Fig. 1, cell survival was increased during the calcination temperature up to 600 °C (at concentrations of 60-600 µg/ml) but then decreased. So that the maximum and minimum relative viability were observed at 600 °C and amorphous. However, the difference between relative viability in A and E was statistically significant only at 60µg / ml ($p = 0.0256$). Because A NPs are amorphous, they have a greater reactivity with MRC-5 due to the high surface area to volume ratio. However, at higher temperatures, due to the regular structure and reduced surface area of nanoparticles, their reaction capacity and catalytic activity have decreased which is effective in reducing their toxicity (14, 33). However, the results indicated that the increase in calcination temperature did not significantly change the degree of crystallization, but, due to the formation of regular crystals at 1000 °C, the maximum toxicity of MRC-5 at concentrations of 600 and 6000 µg/ml was due to exposure to D nanoparticles. In addition, the difference between OD in D and E nanoparticles was significant only at 6000 µg/ml ($P = 0.039$). Pearson's correlation showed that there was a positive correlation with cell proliferation at 600 µg/ml during calcination temperature ($R^2 = 0.78$). However, this correlation was very weak at concentrations of 60 and 6000µg/ml ($R^2_{6000\mu g/ml} = -0.2$; $R^2_{60\mu g/ml} = 0.09$). Thus, in addition to the toxicity of crystalline nanoparticles, amorphous SiO_2 also has high toxicity to MRC-5. In the study of Asad et al., 2018 there was also a negative correlation between high concentrations of 100µg/ml SiO_2 NPs and the cell proliferation of the RD cell line in the 24 h exposure (16). Also during the silica calcification temperature, the trend of cell survival changes at concentration of 60 µg/ml was positively correlated with concentration of 600 µg/ml ($R^2 = 0.5$) while correlation was negative with concentration of 6000 µg/ml ($R^2 = -0.79$ and $R^2 = -0.54$). According to these results, with SiO_2 NP's logarithmic increasing concentration, OD did not increase logarithmically. Therefore, it is necessary to determine the relationship between cellular viability and exposure to different concentrations of SiO_2, as described in Section 3.4. Besides, with increasing crystallization, the difference between OD at different concentrations increased. Concentration is, therefore, an influential factor in cellular viability and exposure to low concentrations of amorphous nanoparticles has been shown to affect cellular viability. Because silica nanoparticles are stable and at low concentrations, they have a high potential for the production of radicals and oxidizing agents. But there is no linear pattern for OD changes in nanoparticles with different crystallization times. Thus, considering the similarity of toxicity rates of 600 and 6000µg/ml of E nanoparticles in MRC-5 and

limited crystallization of other nanoparticles, E nanoparticle was selected and other variables affecting crystallization such as calcination time were investigated.

3.3.2. Toxicity of SiO_2 NPs based on calcination time at 1000°C

The degree of cytotoxicity induced by increasing the calcination time of E nanoparticles at 1000°C also shows that there is no linear pattern for OD changes in nanoparticles with different crystallization times. So that with increasing time, OD increased at 6000 µg/ml concentration. However, the maximum toxicity at concentrations of 60 and 6000 µg/ml in the calcinated nanoparticles was at 12 h.

Also, at a concentration of 100 µg/ml, there was no difference between cell proliferations ($p > 0.05$). As the crystallization of silica nanoparticles increases, the relationship between concentration variables and the degree of crystallization has changed with the degree of cell proliferations, which needs further evaluation.

3.3.3. Toxicity of SiO_2 NPs based on catalyst feed rate at 1000°C

Based on the used method in the synthesis of SiO_2 NPs, details of the cell proliferations of MRC-5 at three concentrations of 42, 420, and 4200 µg/ml are shown in Fig. 3.

As shown in Fig. 3, cell proliferations was different in various feed rates. So the minimum cell proliferations was at feed rate = 0.05 ml/min ($p < 0.05$). Pearson correlation also showed that at 42µg/ml concentration, there was a negative correlation between cell proliferation and feed rate increase ($R^2 = -0.97$). Also, at 0.01 ml/min, the maximum toxicity was at 4200 µg/ml ($p > 0.05$), while at B and C nanoparticles, the minimum cell proliferations was at 42 µg/ml. However, only in C nanoparticles, there was a significant difference between the cell proliferations of different concentrations ($p < 0.05$). Thus, increasing the catalyst feed rate during the nanoparticle synthesis steps is an effective factor in decreasing cell proliferations, and it is suggested that the feed rate decrease. Because, according to SEM results, the change in feed rate did not affect the physicochemical properties of the nanoparticles, such as size, but was effective in inducing nanoparticle toxicity in lung cells.

3.4. Prediction of Cellular Viability using ANN

In this study, cell proliferation in MRC-5 exposed to different concentrations of SiO_2 NPs was first studied by the linear regression model. In Table 3, error rates and correlation coefficients for different concentrations are shown by using the linear regression model.

Table 3. The bias and correlation coefficient of cell proliferation in MRC-5 exposed to various concentration of SiO_2 NPs.

Concentration	R^2	MSE
60 µg/ml	0.05	0.8
100 µg/ml	0.78	0.08
600 µg/ml	0.73	0.12
6000 µg/ml	0.16	0.33

According to Table 3, the cell proliferation was only more consistent with the linear regression model at the concentration of 100 µg/ml (MSE = 0.08, RMSE = 0.26 and R^2 = 0.78). In this way, the artificial neural network method, which is a nonlinear method, is used for predicting and modeling. The Levenberg-Marquardt algorithm for weight and bias was used to determine the best network structure. In this study, based on the number of input and output variables, the number of neurons in the hidden layer = 3 - 10 was used to predict cell proliferations by using ANN, which the best of it was related to 10 neurons, according to Table 5. Because it had the highest correlation coefficient and the lowest MSE for all datasets (0.97) and test datasets (0.98). Figure 4 shows the structure of the best predictive model and the relationship between input and output by the hidden layer. The minimum MSE = 0.003 (Fig. 4a) was also at Epoch = 1, which after this point, overfit data and validation set error began to increase. When the cell proliferations error is increased for seven iterations, the training is stopped based on the stop algorithm. This prevents network overfits. Also, the regression coefficient in Fig. 4b shows that the correlation in test dataset = 0.98 and all test = 0.97. The prediction rate by using ANN compared with the experimental value is shown in Table 4. The maximum and minimum cell proliferation in real samples was 0.1 and 0.001 M, respectively, which was at the calcination temperature of 1000°C with feed rate = 0.01 ml/min and HRT = 2 h at runs 20 and 13, respectively. The results of the ANN prediction were similar, too. In Fig. 5, the correlation between the predicted values by the ANN model versus the actual value obtained from the laboratory tests is 0.94, which indicating a high correlation between the network output and the cell proliferations. Thus, the artificial neural network has the potential to predict cellular viability in MRC-5 cells in the face of different types of amorphous and crystalline nanoparticles at different concentrations. In the study of Rezai et al., 2016, the use of the artificial neural network has also been introduced as a useful, reliable, cheap, and fast tool for predicting lethality in human cancer cells (34).

Table 4. The design matrix of four independent variables for cell proliferation of MRC-5 (the laboratory results and predicted ANN)

Run number	Calcination temperature (°C)	Concentration of SiO_2 NP (µg/ml)	Feed rate of catalyst	HRT (h)	Viability of MRC-5 at OD 570nm	ANN Predicted values
1	70	60	0.01	2	0.736	0.732
2	70	100	0.01	2	0.659	0.721
3	70	600	0.01	2	0.535	0.518
4	70	6000	0.01	2	0.174	0.139
5	350	60	0.01	2	0.781	0.776
6	350	100	0.01	2	0.768	0.769
7	350	600	0.01	2	0.626	0.611
8	350	6000	0.01	2	0.056	0.086
9	600	60	0.01	2	0.803	0.803
10	600	100	0.01	2	0.731	0.797
11	600	600	0.01	2	0.671	0.675
12	600	6000	0.01	2	0.140	0.058
13	**800**	**60**	**0.01**	**2**	**0.943**	**0.821**
14	800	100	0.01	2	0.790	0.817
15	800	600	0.01	2	0.677	0.701
16	800	6000	0.01	**2**	0.154	0.092
17	1000	60	0.01	2	0.73	0.757
18	1000	100	0.01	2	0.774	0.752
19	1000	600	0.01	2	0.642	0.621
20	**1000**	**6000**	**0.01**	**2**	**0.025**	**0.063**
21	1000	60	0.01	12	0.802	0.78
22	1000	100	0.01	12	0.794	0.777
23	1000	600	0.01	12	0.714	0.686
24	1000	6000	0.01	12	0.544	0.524
25	1000	60	0.01	24	0.875	0.798
26	1000	100	0.01	24	0.734	0.794
27	1000	600	0.01	24	0.714	0.704

28	1000	6000	0.01	24	0.622	0.626
29	1000	60	0.01	5	0.731	0.638
30	1000	100	0.01	5	0.641	0.634
31	1000	600	0.01	5	0.473	0.515
32	1000	60	0.05	5	0.138	0.176
33	1000	100	0.05	5	0.211	0.177
34	1000	600	0.05	5	0.18	0.187
35	1000	60	0.1	5	0.231	0.384
36	1000	100	0.1	5	0.541	0.381
37	1000	600	0.1	5	0.469	0.337

Table 5. Number of neurons in hidden layer (3-10 neurons).

Number of neuron in hidden layer	R(all data)	R (test data)	MSE
4:10:1	0.97	0.98	0.003
4:9:1	0.958	0.98	0.0031
4:8:1	0.959	0.96	0.0021
4:7:1	0.915	0.92	0.0015
4:6:1	0.92	0.96	0.021
4:5:1	0.9	0.89	0.015
4:4:1	0.959	0.96	0.027
4:3:1	0.91	0.81	0.0014

4. Conclusion

In this study, the effects of temperature and time of calcination and feed rate of catalyst on the crystallization rate of SiO_2 NPs were investigated, and then their cell proliferations on MRC-5 during 24 h exposure was studied.

The results of the study are shown as follows:

- The size of the synthesized nanoparticles was less than 50 nm in all conditions. Whereas DLS results showed that the primary and secondary size of amorphous nanoparticles changed in aqueous media. Thus, unlike other investigated nanoparticles in this study, amorphous SiO_2 NPs rapidly agglomerated, which can affect its properties (primary diameter <50 nm and secondary diameter> 1000 nm).
- During the calcination temperature up to 1000 ° C, the peak of the XRD diagram changed from 21-30 °, indicating a change in their crystallization. The maximum crystallization rate was observed at 1000 °C, which was 58% higher than amorphous. The EDS results also confirm that with increasing calcinated temperature, the purity of the nanoparticles increased (only Si and O were observed in the crystals). Thus, increasing calcination temperature has been an effective factor in the crystallization of SiO_2
- Nanoparticle crystallization increased with increasing calcination time and reduced feed rate but did not have a significant effect on MRC-5 cell proliferations.
- By increasing the concentration of nanoparticles and increasing the crystalinity of amorphous cells, cell proliferation decreased. Thus, the crystallization of SiO_2 NPs is an effective factor in MRC-5 cell death.
- An increase in calcination temperature was highly correlated (R_2 = 0.78) with cell proliferation at 600 µg/ml concentration, whereas no correlation was observed at other concentrations. Thus, besides to the crystallization of the nanoparticles, the concentration is also an effective factor in MRC-5 cell death.
- Cell proliferation was positively correlated at concentrations of 60 and 600 µg/ml (R^2 = 0.5) while negatively correlated with concentrations of 6000 µg/ml (R^2 = -0.54 and R^2 = -0.79). Consequently, with logarithmic increasing of SiO_2 NPs concentration, no logarithmic decrease in cell proliferation has been observed, which requires the use of other prediction models. Cell proliferation in MRC-5 was slightly correlated with linear regression model (MSE> 0.08 and RMSE = 0.26), but modeling results by using artificial neural network showed that the best structure for this study was 4:10:1 with R^2_{all} = 0.97, R^2_{test} = 0.97, RMSE = 0.25 and MSE = 0.003, and training is stopped in seven iterations due to increased validation error. The correlation between the laboratory results and the ANN prediction was 0.94, in which the minimum and maximum cell proliferation in the laboratory data and the ANN results were reported in the same conditions (run = 20 and 16).

Declarations

Acknowledgment

This project was financially supported by Shiraz University of Medical Sciences, phD thesis of Fariba Abbasi (No. 19159).

Funding

Shiraz University of medical science.

Competing interests

There are no competing interest.

Availability of supporting data

The supporting data are available from the corresponding author on reasonable request.

Ethics approval and consent to participate

All ethical aspects of this study were approved by Shiraz University of medical science' Ethics Committee.

Consent for publication

Not applicable.

Author contribution

FA participated in the design of study, performing experimental, data collection and analysis and write the article. MRS participated the design of study and the main edit of article. HH, AA and MJF participated in the design of study. ASD participated in the design of study and data collection. MJ participated in edit of article. SB participated in edition of article.

References

1. Guo C, Xia Y, Niu P, Jiang L, Duan J, Yu Y, et al. Silica nanoparticles induce oxidative stress, inflammation, and endothelial dysfunction in vitro via activation of the MAPK/Nrf2 pathway and nuclear factor-κB signaling. International journal of nanomedicine. 2015;10:1463.
2. Zainuri M. Synthesis of SiO2 nanopowders containing quartz and cristobalite phases from silica sands. Materials Science-Poland. 2015;33(1):47-55.
3. Ma X, Jian R, Chang PR, Yu J. Fabrication and characterization of citric acid-modified starch nanoparticles/plasticized-starch composites. Biomacromolecules. 2008;9(11):3314-20.
4. Soltani M, Lin J, Forties RA, Inman JT, Saraf SN, Fulbright RM, et al. Nanophotonic trapping for precise manipulation of biomolecular arrays. Nature nanotechnology. 2014;9(6):448.
5. Hori N, Iwasa F, Ueno T, Takeuchi K, Tsukimura N, Yamada M, et al. Selective cell affinity of biomimetic micro-nano-hybrid structured TiO2 overcomes the biological dilemma of osteoblasts. Dental Materials. 2010;26(4):275-87.
6. Bettermann P, Liebau F. The transformation of amorphous silica to crystalline silica under hydrothermal conditions. Contributions to Mineralogy and Petrology. 1975;53(1):25-36.

7. Fuchs I, Aluma Y, Ilan M, Mastai Y. Induced crystallization of amorphous biosilica to cristobalite by silicatein. The Journal of Physical Chemistry B. 2014;118(8):2104-11.
8. Tanyildizi H. Statistical analysis for mechanical properties of polypropylene fiber reinforced lightweight concrete containing silica fume exposed to high temperature. Materials & Design. 2009;30(8):3252-8.
9. Kazemi A, Faghihi-Sani M, Alizadeh H. Investigation on cristobalite crystallization in silica-based ceramic cores for investment casting. Journal of the European Ceramic Society. 2013;33(15-16):3397-402.
10. Guichard Y, Fontana C, Chavinier E, Terzetti F, Gate L, Binet S, et al. Cytotoxic and genotoxic evaluation of different synthetic amorphous silica nanomaterials in the V79 cell line. Toxicology and industrial health. 2016;32(9):1639-50.
11. Uboldi C, Giudetti G, Broggi F, Gilliland D, Ponti J, Rossi F. Amorphous silica nanoparticles do not induce cytotoxicity, cell transformation or genotoxicity in Balb/3T3 mouse fibroblasts. Mutation Research/Genetic Toxicology and Environmental Mutagenesis. 2012;745(1-2):11-20.
12. Maser E, Schulz M, Sauer UG, Wiemann M, Ma-Hock L, Wohlleben W, et al. In vitro and in vivo genotoxicity investigations of differently sized amorphous SiO2 nanomaterials. Mutation Research/Genetic Toxicology and Environmental Mutagenesis. 2015;794:57-74.
13. Friedman A, Blecher K. Nanotechnology in the treatment of infectious diseases. Nanotechnology in Dermatology: Springer; 2013. p. 187-200.
14. Murugadoss S, Lison D, Godderis L, Van Den Brule S, Mast J, Brassinne F, et al. Toxicology of silica nanoparticles: an update. Archives of toxicology. 2017;91(9):2967-3010.
15. Rabolli V, Thomassen LC, Uwambayinema F, Martens JA, Lison D. The cytotoxic activity of amorphous silica nanoparticles is mainly influenced by surface area and not by aggregation. Toxicology letters. 2011;206(2):197-203.
16. Petrache Voicu S, Dinu D, Sima C, Hermenean A, Ardelean A, Codrici E, et al. Silica nanoparticles induce oxidative stress and autophagy but not apoptosis in the MRC-5 cell line. International journal of molecular sciences. 2015;16(12):29398-416.
17. Chen L, Liu J, Zhang Y, Zhang G, Kang Y, Chen A, et al. The toxicity of silica nanoparticles to the immune system. Nanomedicine. 2018;13(15):1939-62.
18. Gonçalves M. Sol-gel silica nanoparticles in medicine: A natural choice. Design, synthesis and products. Molecules. 2018;23(8):2021.
19. Blagojev N, Kukić D, Vasić V, Šćiban M, Prodanović J, Bera O. A new approach for modelling and optimization of Cu (II) biosorption from aqueous solutions using sugar beet shreds in a fixed-bed column. Journal of hazardous materials. 2019;363:366-75.
20. Mohammadi F, Samaei MR, Azhdarpoor A, Teiri H, Badeenezhad A, Rostami S. Modelling and optimizing pyrene removal from the soil by phytoremediation using response surface methodology, artificial neural networks, and genetic algorithm. Chemosphere. 2019;237:124486.

21. Gharagozlou M. Influence of calcination temperature on structural and magnetic properties of nanocomposites formed by Co-ferrite dispersed in sol-gel silica matrix using tetrakis (2-hydroxyethyl) orthosilicate as precursor. Chemistry Central Journal. 2011;5(1):19.
22. Waseem M, Mustafa S, Naeem A, Shah K, Shah I, Haque I. Synthesis and characterization of silica by sol-gel method. J Pak Mater Soc. 2009;3:19.
23. Rovani S, Santos JJ, Coriob P, Fungaroa DA. An Alternative and Simple Method for the Preparation of Bare Silica Nanoparticles Using Sugarcane Waste Ash, an Abundant and Despised Residue in the Brazilian Industry. J Braz Chem Soc. 2019;30(7):1524-33.
24. Muljani S, Wahyudi B, Sumada K, editors. Potassium Silicate Foliar Fertilizer Grade from Geothermal Sludge and Pyrophyllite. MATEC Web of Conferences; 2016: EDP Sciences.
25. Metcalf, Eddy. Wastewater engineering: collection, treatment, disposal: McGraw-Hill; 1972.
26. Mori D, Oyama Y, Hirose T, Muro T, Matsui F. Local structural determination of N at SiO2/SiC (000 1^{-}) interfaces by photoelectron diffraction. Applied Physics Letters. 2017;111(20):201603.
27. Wahab R, Khan F, Gupta A, Wiggers H, Saquib Q, Faisal M, et al. Microwave plasma-assisted silicon nanoparticles: cytotoxic, molecular, and numerical responses against cancer cells. RSC Advances. 2019;9(23).
28. Orives JR, Viali WR, Magnani M, Nalin M. Incorporation of CdFe2O4-SiO2 nanoparticles in SbPO4-ZnO-PbO glasses by melt-quenching process. Eclética Química. 2018;43(2):32-43.
29. Wang Y, Zhang X, Liu Y, Jiang Y, Zhang Y, Yang J. Microstructure and magnetic properties of L1 0 CoPt nanoparticles by Ag addition. Journal of Sol-Gel Science and Technology. 2014;70(3):528-33.
30. Ahamed M. Silica nanoparticles-induced cytotoxicity, oxidative stress and apoptosis in cultured A431 and A549 cells. Human & experimental toxicology. 2013;32(2):186-95.
31. Rismanchian M, Khodaeian N, Bahramian L, Fathi M, Sadeghi-Aliabadi H. In-vitro comparison of cytotoxicity of two bioactive glasses in micropowder and nanopowder forms. Iranian journal of pharmaceutical research: IJPR. 2013;12(3):437.
32. China C. ZnO, TiO 2, SiO 2, and Al 2 O 3 Nanoparticles-induced Toxic Effects on Human Fetal Lung Fibroblasts* ZHANG X iao Qiang, YIN L i Hong, TANG Meng, and PU Y ue Pu 1. School of Public Health, Southeast University, Nanjing 210009, Jiangsu, China; 2. Key Laboratory of Environmental Medicine and Engineering, Ministry of Education, Southeast University, Nanjing 210009, Jiangsu, China. Biomed Environ Sci. 2011;24(6):661-9.
33. Sukhanova A, Bozrova S, Sokolov P, Berestovoy M, Karaulov A, Nabiev I. Dependence of nanoparticle toxicity on their physical and chemical properties. Nanoscale research letters. 2018;13(1):44.
34. Rezaei A, Noori L, Taghipour M. The use of ANFIS and RBF to model and predict the inhibitory concentration values determined by MTT assay on cancer cell lines. International Journal of Information Technology and Computer Science (IJITCS). 2016;8(4):28-34.

Figures

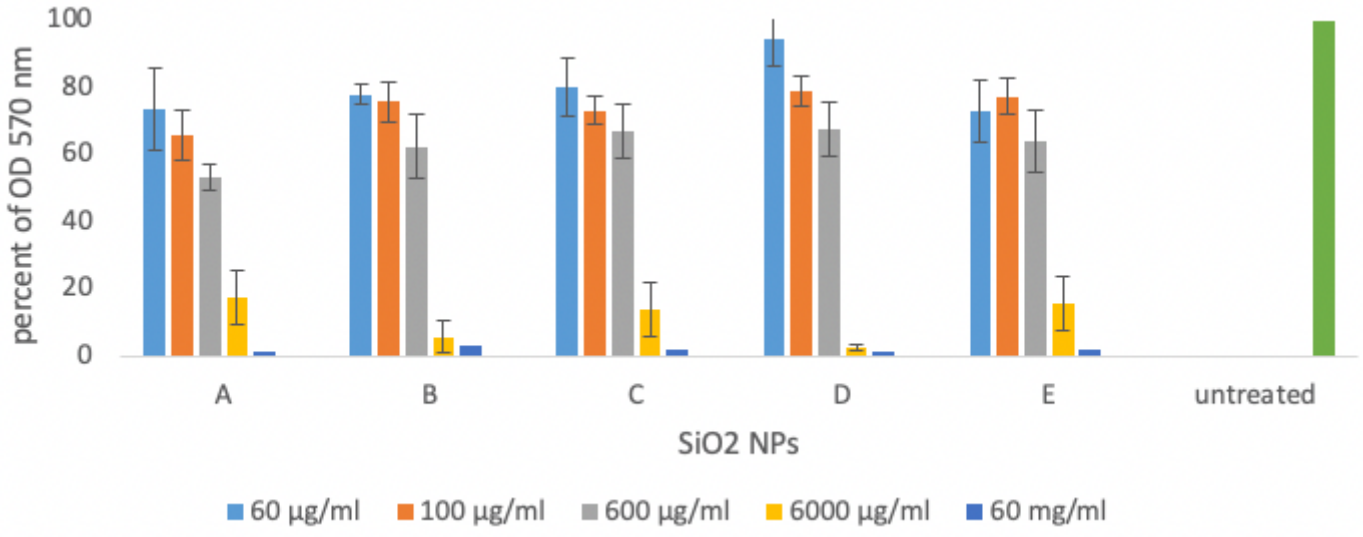

Figure 1

Toxicity of SiO2 NPs on cell proliferation of MRC-5 exposed during 24h to SiO2 NPs. A: amorphous SiO2, B: SiO2 NPs calcinated at 350°C, C: SiO2 NPs calcinated at 600°C, D: SiO2 NPs calcinated at 800°C, E: SiO2 NPs calcinated at 1000°C.

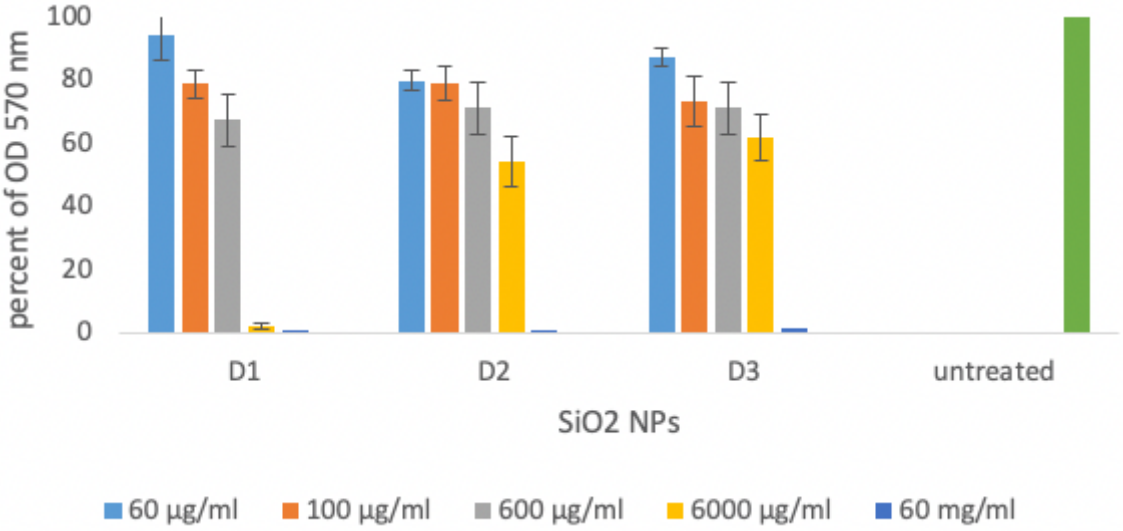

Figure 2

Toxicity of SiO2 NPs on cell proliferation of MRC-5 at 1000°C during D1) 2h, D2) 12h and D3) 24 h.

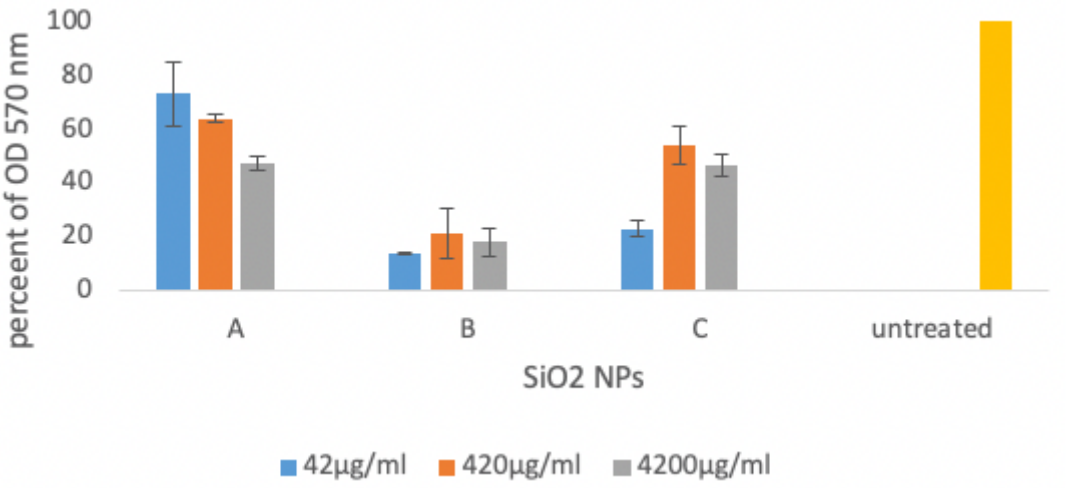

Figure 3

Toxicity of SiO2 NPs on cell proliferation of MRC-5 at 1000°C during various feed rate of catalyst. A) Feed rate = 0.01 ml/min, B) feed rate = 0.05 ml/min and C) feed rate = 0.1 ml/min.

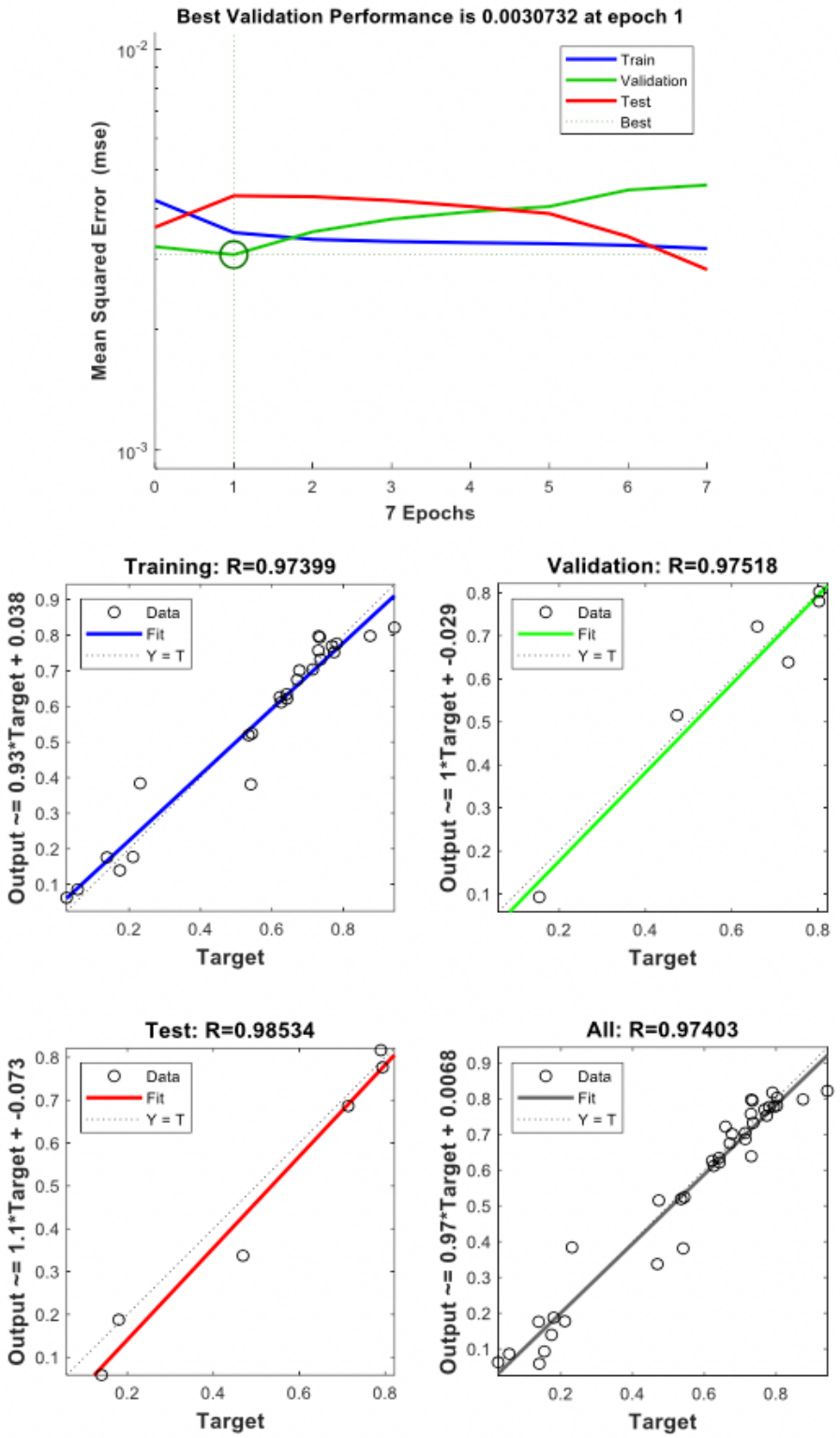

Figure 4

The structure of best model for prediction of cellular proliferation related to calcination temperature

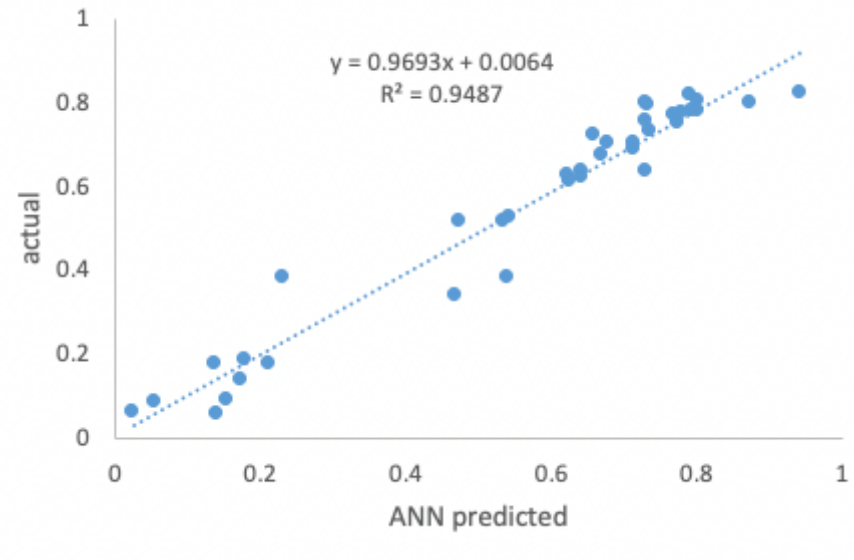

Figure 5

Cell proliferation of MRC-5 exposed to SiO2 NPs for the actual laboratory results and the predicted by ANN model.